Melting behavior of the β-Pb/Ge(111) structure

M. F. Reedijk,[1] J. Arsic,[1] D. Kaminski,[1] P. Poodt,[1] H. Knops,[2] P. Serrano,[3] G. R. Castro,[3] and E. Vlieg[1]
[1]*NSRIM Department of Solid State Chemistry, University of Nijmegen, Toernooiveld 1, 6525 ED Nijmegen, The Netherlands*
[2]*Institute of Theoretical Physics, University of Nijmegen, Toernooiveld 1, 6525 ED Nijmegen, The Netherlands*
[3]*SpLine at ESRF, BP220, F-38043 Grenoble Cedex, France*
(Received 30 September 2002; published 29 April 2003)

The two-dimensional phase transition of the $(\sqrt{3}\times\sqrt{3})$ $R30°$-Pb/Ge(111) surface is analyzed using surface x-ray diffraction. The critical exponents β, ν, and γ have been determined. These exponents exhibit mean-field behavior indicating a long-range interaction potential for the Pb atoms. Deviations from the mean-field behavior, due to finite-size effects, occur at temperatures close to T_c.

DOI: 10.1103/PhysRevB.67.165423 PACS number(s): 68.08.De, 68.15.+e, 68.18.Jk

I. INTRODUCTION

The nature of the two-dimensional (2D) melting transition has received considerable attention because the character of this transition in two dimensions is different from the melting in three dimensions. Critical fluctuations play a more important role in melting in lower dimensions. The melting transition is always a first-order process in a bulk solid, but it can be continuous, or even of infinite order, in a 2D layer. This was pointed out by Kosterlitz and Thouless[1] for a free floating surface, where the long-range orientation order is broken at the transition temperature. Several years later the ideas were extended by Halperin, Nelson, and Young.[2] In the presence of a (crystalline) substrate where long-range translational order is present, the 2D phase transitions can be grouped in a few universality classes, such as the Ising and Potts models,[3] based on the symmetry of the system. These models predict the nature of the order-disorder transition and the critical exponents. Experimental validation of the theories is limited, because the investigated systems are never completely two dimensional. Typical pseudo-two-dimensional systems are monolayers supported on a substrate or crystal surface.[4–7] The samples have to be as perfect as possible, since defects and steps can easily influence the critical behavior.[8]

We have studied the nature of the ''2D'' melting transition of a lead monolayer (ML) on Ge(111), which is a convenient model system.[9] The mutual solid solubility is negligible and the system forms a well defined interface. In addition, lead has a low melting point as well as a low vapor pressure. The phase diagram of the Pb/Ge(111) system has been extensively studied.[9,10] We recently proposed a modification at high coverages.[11] Two stable $(\sqrt{3}\times\sqrt{3})$ $R30°$ ($\sqrt{3}$ in short) phases can be formed on the surface, a low-density α phase at $\frac{1}{3}$ ML and a dense β phase, which is stable at coverages between 1.25 and $\frac{4}{3}$ ML. Here 1 ML is equal to a single Ge(111) layer (half a bilayer), so $\frac{1}{3}$ and $\frac{4}{3}$ ML correspond to one and four atoms per $\sqrt{3}$ unit cell, respectively. The α phase has a transition temperature near 400 °C. At this temperature the desorption rate of Pb of the surface is so high that experiments are very difficult. The melting temperature of the β phase depends critically on the coverage, ranging from 180 to 270 °C. When more than $\frac{4}{3}$ ML of Pb is deposited on the surface a metastable β' phase forms.[11] This phase has a structure which closely resembles the structure of the β phase, but the excess Pb on the surface pins this structure and prevents it from melting. Here, we focus on the 2D phase transition of the β phase. Because this system has three equivalent $\sqrt{3}$ domains, it is expected to fall in the Potts universality class with $q=3$.

The structures of both the solid and the molten β phase have been investigated by several groups.[9–11] It has been found that the ''liquid'' phase at a coverage around 1.25 ML's has both solid and liquid character. The Pb atoms spend a significant fraction of their time close to lattice sites. Previous experiments on this system showed a peak broadening close to the transition temperature indicating a continuous transition, but the corresponding critical exponents were not determined.[9,10]

Here, we report an experimental analysis of the critical exponents β, ν, and γ of the melting transition of the β-Pb/Ge(111) system. The critical exponents are determined using surface x-ray diffraction (SXRD), which is very suitable to probe the long- and short-range order of the system. We show that the $\sqrt{3}\rightarrow(1\times1)$ phase transition is indeed continuous. However, the critical exponents measured do not correspond to the expected three-state Potts exponents; instead they show a typical mean-field behavior.

II. EXPERIMENT

The SXRD experiments were performed in an ultrahigh vacuum environment (UHV) on the DUBBLE beamline (ESRF, Grenoble).[12] The setup consists of a UHV chamber which was modified to fit on the $2+3$ circle diffractometer.[13,14] The base pressure of the system was 3×10^{-10} mbar, during the surface preparation the pressure never exceeded 1×10^{-9} mbar. All data were measured at a wavelength of 1.13 Å, with a constant incoming angle of 1°. The Ge(111) sample was heated using a filament, while the temperature stability was monitored using a thermocouple. The temperature was derived using the power of the filament, which was calibrated against the bulk Pb melting point. The absolute error in the critical temperature is ±10 K, but the relative error ±1 K.

To denote the surface structure, we use a 1×1 surface unit cell for Ge(111), whose lattice vectors are expressed in terms of the conventional cubic lattice by $\mathbf{a}_1=\frac{1}{2}[10\bar{1}]$, $\mathbf{a}_2$

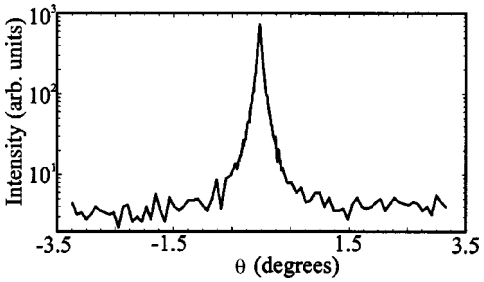

FIG. 1. Rocking scan of the $(\frac{2}{3}, \frac{2}{3}, 0.3)$ reflection at 440 K. The log scale shows the very long tails of the Lorentzian line profile.

$=\frac{1}{2}[\bar{1}10]$, and $\mathbf{a}_3=\frac{1}{2}[111]$. The coordinates are in units of the germanium lattice constant (5.66 Å at 300 °K). The corresponding reciprocal-lattice vectors $\mathbf{b}_i$ are defined by $\mathbf{a}_i \cdot \mathbf{b}_j = 2\pi\delta_{ij}$. The momentum transfer $\mathbf{Q}$, which is the difference between the incoming and outgoing wave vectors, is denoted by the diffraction indices *hkl* in reciprocal space: $\mathbf{Q}=h\mathbf{b}_1 + k\mathbf{b}_2 + l\mathbf{b}_3$. The indices (*hk*) refer to the in-plane component of the momentum transfer and *l* to the perpendicular component.

The polished Ge(111) crystals were cleaned using repeated cycles of sputtering and annealing until a $c(2\times8)$ reconstruction was observed. The miscut of the crystals was ~0.2°, which corresponds to an average terrace width of ~900 Å. A Knudsen effusion cell was used for the deposition of Pb. The deposition rate was calibrated by observing a diffraction peak from the $\sqrt{3}$ reconstruction, and was typically 0.03 ML/min. The $\sqrt{3}$-Pb/Ge surface is obtained as follows. First a little over $\frac{4}{3}$ ML Pb is deposited on the surface at 230 °C, which is above the lowest transition point at 180 °C but below the melting point of the β phase, resulting in a metastable β' phase.[11] Subsequently this phase is annealed at 330 °C and cooled to room temperature, resulting in a β phase with a coverage of 1.28 ML's (in the two-dimensional layer). At this point the surface consists of a two-dimensional Pb layer having a β structure and a few large three-dimensional Pb islands. The total coverage is still above $\frac{4}{3}$ ML. There appears to be no exchange between the Pb islands and the surface, because the coverage in the two-dimensional layer does not reach the value of $\frac{4}{3}$ ML for the ideal β phase.[11]

To obtain the critical exponents, the $(\frac{2}{3}, \frac{2}{3}, 0.3)$ reflection is monitored over a wide temperature range. This reflection originates exclusively from the two-dimensional $\sqrt{3}$ surface, thus the three-dimensional islands are ignored. Measurements are performed at both increasing and decreasing temperatures and on different samples and preparations. At every temperature the surface was allowed to equilibrate until no changes in peak height and width were observed and the thermocouple showed a stable readout. Wide rocking scans (±3.5°) are performed to obtain accurate background information and the detector slits were set fully open (±0.2°) in order to obtain a fairly complete integration in this direction (a full integration of the Lorentzian line shapes is nearly impossible).[15] A typical example of a rocking scan is shown in Fig. 1.

III. DATA ANALYSIS

At low temperatures the β-Pb/Ge(111) surface consists of three equivalent $\sqrt{3}$ domains with equal occupancy and with a domain size that is limited by defects and steps. This is the longest length scale in our system. When approaching the melting point, small domains develop within the large domains. At the critical temperature the small domains form a connected network, while the initial long-range-order domains have disappeared. The small domains give rise to critical scattering, which reaches a maximum at the critical temperature and vanishes at higher temperatures.

Thus the total scattering $S(q,t)$ consists of a long-range order, a critical scattering, and a background scattering term:

$$S(q,t)=I_{\mathrm{long}}(t)F_{\mathrm{long}}(q)+F_{\mathrm{crit}}(t,q)+I_{\mathrm{bg}}. \qquad (1)$$

Here q is the distance to the measured fractional-order reflection and $t=|T-T_c|$ is the difference from the critical temperature T_c. The first term, describing the long-range order, is the product of an intensity $I_{\mathrm{long}}(t)$ with a line shape $F_{\mathrm{long}}(q)$. In this case of three equivalent domains and a measurement of a fractional-order reflection, the line shape is expected to be Lorentzian,[16] and that is indeed what we find. There is no true long-range order; the constant peak width is determined by steps and defects. For a continuous transition $I_{\mathrm{long}}(t)$ behaves like $\sqrt{I_{\mathrm{long}}}\propto t^{\beta}$, where β is the critical exponent of the order parameter. At temperatures above T_c, $I_{\mathrm{long}}=0$.

The second term describes the short-range fluctuations, i.e., the critical scattering. Above T_c, this is the only remaining term, apart from the background scattering I_{bg}. The critical scattering is approximated with a Lorentzian line shape,

$$F_{\mathrm{crit}}(q,t)=\chi(t)\frac{1}{\sigma^2+4q^2}, \qquad (2)$$

where $\chi(t)$ denotes the susceptibility and σ is the full width at half maximum (FWHM), which is inversely proportional to the correlation length ξ. The susceptibility depends on the critical exponent γ, according to $\chi=\chi_0|t|^{-\gamma}$, while the correlation length behaves like $\xi=\xi_0|t|^{-\nu}$.

At $T\ll T_c$ the critical scattering can be neglected and the only term contributing to the scattering is the long-range-order term with a single Lorentzian line shape. The width of the profile remains constant and is fixed at the low-temperature value during the fitting procedure. Figure 2(a) shows a typical example of such an experimental curve. Figure 2(b) shows a profile at a temperature just below T_c. Here both terms contribute to the scattering. This profile can be fitted with a two-component line shape, a sharp peak for the long-range order (with a fixed width) and a wider peak for the critical scattering. At temperatures above T_c, the critical scattering is the only remaining contribution [Fig. 2(c)] and the experimental profile can again be fitted with a single Lorentzian.

This analysis of the experimental profiles resulted in a data set of I_{long}, χ, and σ as a function of temperature. To obtain the corresponding critical exponents β, γ, and ν these order parameters are fitted simultaneously. The temperature

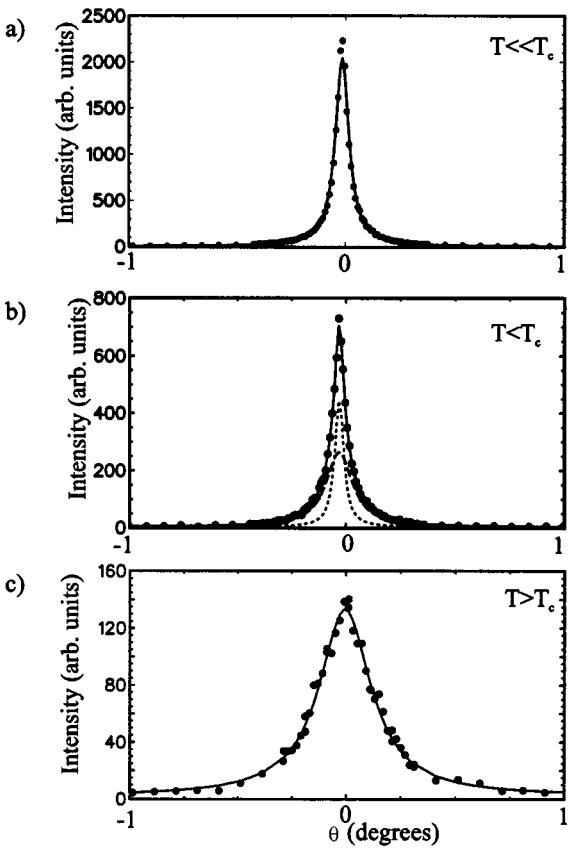

FIG. 2. Broadening of the $(\frac{2}{3}, \frac{2}{3}, 0.3)$ reflection at different temperatures. (a) The profile measured at $T=440$ K (dots), which is equal to $F_{\text{long}}(q)$. The solid curve is a Lorentzian fit. (b) Profile measured below T_c at 510 K, the solid line is a fit composed of two Lorentzian line shapes, the long-range-order contribution (dotted line) and the critical scattering (dashed line). (c) Profile measured above T_c at 526 K, where only the critical scattering is present, the solid line is a single Lorentzian fit.

T_c is included as a fit parameter. The experiments are performed at a constant coverage of 1.28 ML's. The excess Pb available on the surface was found not to be in equilibrium with the two-dimensional lead monolayer,[11] and thus the experiments are not performed at constant chemical potential μ. Therefore the exponents measured are effective exponents and they have to be Fisher renormalized,[17]

$$\beta_n=\frac{\beta}{1-\alpha},\quad \nu_n=\frac{\nu}{1-\alpha},\quad \text{and}\quad \gamma_n=\frac{\gamma}{1-\alpha}. \tag{3}$$

where α is the specific-heat exponent, which equals $\frac{1}{3}$ in the case of a three-state Potts model and 0 in case of mean-field behavior.

IV. RESULTS AND DISCUSSION

The resulting values for I_{long}, χ, and σ are plotted in Fig. 3 and show the expected behavior at the phase transition. I_{long} drops to zero at T_c, while the susceptibility shows a peak at the transition temperature where σ has a minimum. The scatter (and thus the error) in the values is quite small, demonstrating that the data are good enough to reliably decompose the profiles in two Lorentzians. In earlier experiments on different systems the critical scattering below T_c was never observed.[4–7] The value found for the width of $F_{\text{long}}(q)$ is 0.05°, which corresponds to a domain size of 1100 Å. The critical temperature found in the fit procedure was 520 ± 10 K.

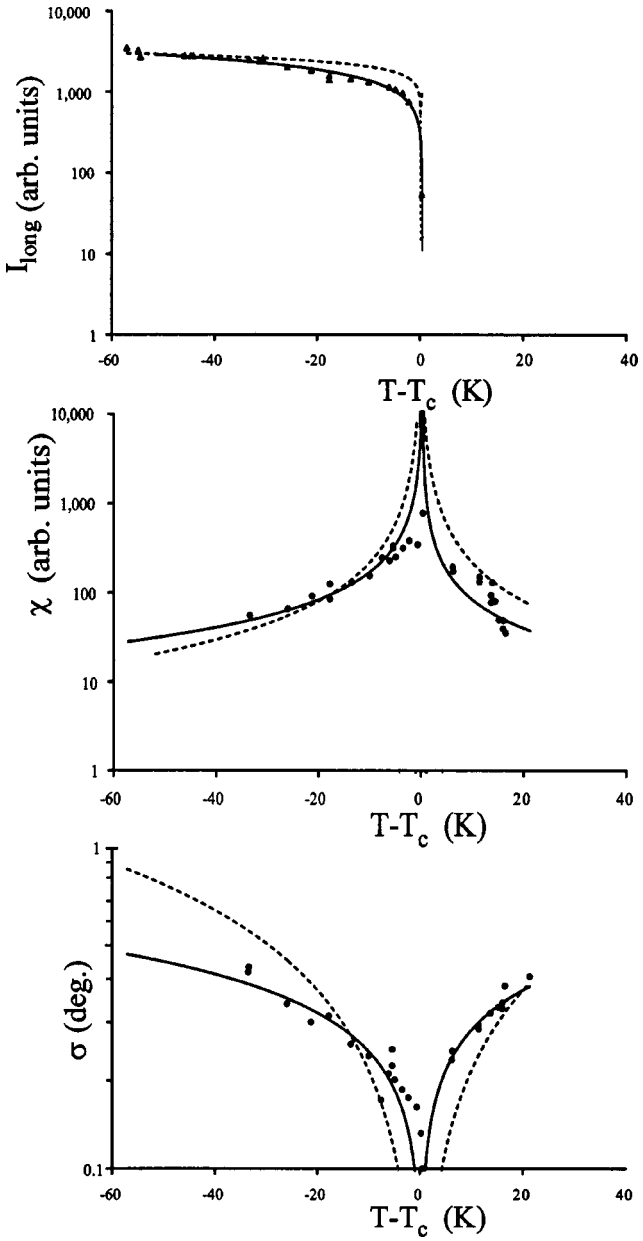

FIG. 3. I_{long} (top), χ (middle), and σ (bottom) plotted on a log scale as a function of the temperature difference $T-T_c$. The critical temperature T_c is 520 K. The solid lines are best-fit calculations giving values of $\beta=0.23$, $\nu=0.51$, and $\gamma=1.05$. The dashed lines are calculations with fixed three-state Potts exponents.

Theoretically, the susceptibility and correlation length diverge at T_c, resulting in a δ profile, but in practice these values are bound by finite-size effects. To eliminate these effects the data for χ and σ at an interval ΔT around T_c are omitted from the fit. The value for ΔT was determined by increasing it until no changes in γ, ν, and T_c were found.

TABLE I. Theoretical and experimental values for the critical exponents. The best-fit values are calculated omitting the data close to T_c (see text).

	ν	γ	β
Best fit	0.51(3)	1.05(5)	0.48(4)[a]
Finite-size convolution	0.44(3)	0.90(5)	
Three-state Potts model	$\frac{5}{6}\approx 0.83$	$\frac{13}{9}\approx 1.44$	$\frac{1}{9}\approx 0.11$
Three-state Potts model, Fisher renormalized	$\frac{5}{4}=1.25$	$\frac{13}{6}=2.17$	$\frac{1}{6}\approx 0.17$
Mean-field model	0.5	1	0.5

[a]When the data close to T_c is included a value of $\beta=0.23$ is found.

This yielded $\Delta T=\pm 5$ K. The values of γ and ν determined by this procedure were 1.05 and 0.51, respectively. Figure 3 shows the corresponding best fits (solid lines). The data for χ deviate at high temperatures, which is probably due to desorption of Pb from the surface.

Omitting the data near T_c is a rather crude, but often used,[8,18,19] way to correct for finite-size effects. The precise consequences of finite-size effects are not known for this system, but to some extent we may account for these effects by convoluting the critical scattering with a profile representing the finite-size effects. While also imperfect, this yields an alternative method to derive the critical exponents and thus provides an additional error estimate as well. At T_c the theoretical profile of $F_{\rm crit}$ is a δ function, and thus the measured profile at T_c yields the width and height of the finite-size smearing function. For convenience, we then use the following relations:

$$\frac{1}{\chi_{\rm exp}}=\frac{1}{\chi_{\rm th}}+\frac{1}{\chi_{\rm fin.\ size}}, \tag{4}$$

$$\sigma^2_{\rm exp}=\sigma^2_{\rm th}+\sigma^2_{\rm fin.\ size}, \tag{5}$$

where $\chi_{\rm exp}$ and $\sigma_{\rm exp}$ are the measured values, $\chi_{\rm th}$ and $\sigma_{\rm th}$ are the values expected theoretically, and where $\chi_{\rm fin.\ size}$ and $\sigma_{\rm fin.\ size}$ take into account the finite-size effects. From the profile at T_c, we find $\chi_{\rm fin.\ size}=800$ and $\sigma_{\rm fin.\ size}=0.1°$. Using this, we find for the critical exponents $\nu=0.44$ and $\gamma=0.90$. In the course of the analysis, we have also calculated the results of using a convolution of two Lorentzians or of two Gaussians, and found that the critical exponents are similar to the ones obtained from the simple method.

The critical exponents ν and γ show large deviations from the values expected for the three-state Potts model; see Table I. For comparison, a fit is shown in Fig. 3 with fixed Potts exponents (dashed lines). Instead, the values found for ν and γ are close to the values expected for mean-field behavior.

The exponent β is derived from the $I_{\rm long}$ data. When all data, including the points near T_c, is included, we find $\beta=0.23$. This does not agree with the three-state Potts model (see Fig. 3), but also not with the mean-field value of $\beta=0.5$. In order to explore the behavior of $I_{\rm long}$, the data are plotted on a linear scale as function of t in Fig. 4. This representation should result in linear behavior in case of mean-field behavior. The data indeed follow a straight line at temperature differences larger than 4 K, but deviations occur at temperatures closer to T_c. Note that this is the same range as estimated for the finite-size effects in the other exponents. When these data are omitted from the fit a value of $\beta=0.48\pm 0.04$ is found, which agrees with the mean-field model. Table I summarizes the exponents found using the different methods.

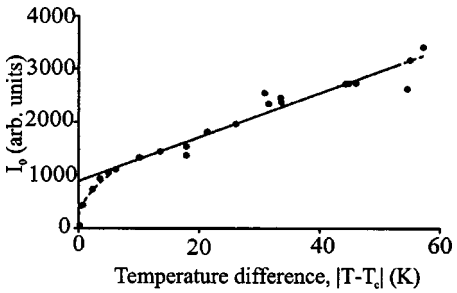

FIG. 4. Peak height of $I_{\rm long}$ vs t. The data follow a straight line (solid line) showing mean-field behavior, but close to T_c a deviation from this line is visible. The dashed line is a fit of the complete data, including the data close to T_c giving a β exponent of 0.23.

Apparently, the long-range scattering and the critical scattering data exhibit a mean-field-like behavior when data close to T_c are omitted. This implies that for such temperatures we are in a regime where the correlation length $\xi(T)$ is smaller than both the system size L and the effective potential range R. This points to a rather long-range interaction between the Pb atoms, which is compatible with the high density of Pb atoms in this phase.[10,11] Possibly, the Pb atoms on the surface have such an interaction owing to the formation of covalent chains.[20] When temperatures closer than 4 K to T_c are included a difference between the critical scattering data and the long-range scattering data is observed. For critical scattering the exponents ν and γ directly cross over from mean-field to finite-size behavior. This suggests that for these temperatures and data one has $\xi(T)\approx L<R$. On the other hand, the long-range scattering data, when analyzed close to T_c, yield an exponent $\beta=0.23$, which is in between the values expected for mean-field (0.5) and the three-state Potts model (0.17 when Fisher renormalized). Apparently the effective potential range $\tilde{R}$ for the order parameter is different in such a way that the inequality above is replaced by $\xi(T)\approx L\approx\tilde{R}$.

It would be interesting to compare the critical exponents of the β phase with those of the α phase. This phase has a low density with a coverage of $\frac{1}{3}$ ML, and does not show metallic behavior at temperatures above 213 K.[21] Similar behavior has been observed for the He-graphite system, where, depending on the preparation, both mean-field[22] and three-state Potts[23] values for the exponent α were found. However, due to the higher transition temperature of the α-Pb/Ge(111) structure, the measurement of these exponents is very difficult.

V. CONCLUSIONS

We have examined the 2D phase transition of the $\sqrt{3}$-Pb/Ge(111) phase. The exponents correspond to the values ex-

pected for mean-field behavior. Deviations for the susceptibility and correlation length occur at temperatures close to the critical temperature, which are due to finite-size effects. The data for I_{long} show a deviation close to T_c, which is probably due to a crossover from mean-field behavior to three-state Potts behavior. The mean-field behavior of the surface shows that the atoms have a long-range interaction potential.

ACKNOWLEDGMENTS

We thank the staff of the DUBBLE beamline at the European Synchrotron Radiation Facility for their assistance during the measurements and I. Cerjak and M. Borsboom for modifying EXODUS. This work is part of the research program of the Foundation for Fundamental Research on Matter (FOM), and was made possible by financial support from the Netherlands Organization for Scientific Research (NWO).

[1] J. M. Kosterlitz and D. J. Thouless, J. Phys. C **6**, 118 (1973).
[2] D. R. Nelson, *Phase Transitions and Critical Phenomena* (Academic, London, 1983), Vol. 7.
[3] M. Schick, Prog. Surf. Sci. **11**, 245 (1981).
[4] M. Sokolowski and H. Pfnur, Phys. Rev. B **49**, 7716 (1994).
[5] D. E. Clark, W. N. Unertl, and P. H. Kleban, Phys. Rev. B **34**, 4379 (1986).
[6] I. K. Robinson, E. Vlieg, and K. Kern, Phys. Rev. Lett. **63**, 2578 (1989).
[7] I. K. Robinson, A. A. MacDowell, M. Altman, P. Estrup, K. Evans-Lutterodt, J. D. Brock, and R. J. Birgeneau, Phys. Rev. Lett. **62**, 1294 (1989).
[8] M. Sokolowski and H. Pfnur, Phys. Rev. Lett. **63**, 183 (1989).
[9] F. Grey, Ph.D. thesis, Copenhagen University, Copenhagen, 1988.
[10] S. A. de Vries, P. Goedtkindt, P. Steadman, and E. Vlieg, Phys. Rev. B **59**, 13 301 (1999).
[11] M. F. Reedijk, J. Arsic, D. Kaminski, P. Poodt, J. W. M. van Kessel, W. J. Szweryn, H. Knops, and E. Vlieg, Phys. Rev. Lett. **90**, 056104 (2003).
[12] M. Borsboom, W. Bras, I. Cerjak, D. Detollenaere, D. G. van Loon, P. Goedtkindt, M. Konijnenburg, P. Lassing, Y. Levine, B. Munneke, *et al.*, J. Synchrotron Radiat. **5**, 518 (1998).
[13] E. Vlieg, A. van't Ent, A. P. de Jongh, H. Neerings, and J. F. van der Veen, Nucl. Instrum. Methods Phys. Res. A **262**, 522 (1987).
[14] E. Vlieg, J. Appl. Crystallogr. **31**, 198 (1998).
[15] E. Vlieg, J. Appl. Crystallogr. **30**, 532 (1997).
[16] E. Vlieg, J. F. van der Veen, S. J. Gurman, C. Norris, and J. E. Macdonald, Surf. Sci. **210**, 301 (1989).
[17] M. E. Fisher, Phys. Rev. **176**, 257 (1968).
[18] I. K. Robinson, E. Vlieg, and K. Kern, Faraday Discuss. Chem. Soc. **89**, 159 (1990).
[19] L. Floreano, D. Cvetko, G. Bavdek, M. Benen, and A. Morgante, Phys. Rev. B **64**, 075405 (2001).
[20] F. Ancilotto, A. Selloni, and R. Car, Phys. Rev. Lett. **71**, 3685 (1993).
[21] J. M. Carpinelli, H. H. Weitering, M. Bartkowiak, R. Stumpf, and E. W. Plummer, Phys. Rev. Lett. **79**, 2859 (1997).
[22] M. J. Tejwani, O. Ferreira, and O. E. Vilches, Phys. Rev. Lett. **44**, 152 (1980).
[23] M. Bretz, Phys. Rev. Lett. **38**, 501 (1977).